DTU Library

Spread of fluid: Role of tip configurations in needles

Gomes, Silvana; Drakidis, Alexandros Dimitrios; Silva, Patricia; Lenau, Torben Anker

Published in:
Skin Research and Technology

Link to article, DOI:
10.1111/srt.12419

Publication date:
2018

Document Version
Peer reviewed version

Spread of fluid: Role of tip configurations in needles

Silvana Gomes[a], Alexandros Drakidis[a], Patricia Silva[a], Torben A.Lenau[a]
[a] Technical University of Denmark, Dept. of Mechanical Engineering,
Produktionstorvet b. 426B DK-2800 Kgs. Lyngby, Denmark.

Background/purpose: During the injection of a fluid in a tissue model, the fluid might be affected by the needle tip configuration and the number of channels. Thus, the objective of the present work is to observe the influence of different needle tips and number of channels on the spread of a fluid.

Methods: Fluid distribution data were obtained after injecting 0.3 ml of fluid into a foamed polymer model with a velocity of 2mm/s. The spread area and the depth were determined for 3 different types of hypodermic needles: Single channel needles with bevel tip and blunt tip and a needle with conical tip and 3 internal channels.

Results: The bevel tip provides a higher spread in the direction where the bevel points and reaches larger depths than the other two needles. The spread for the blunt tip and the polymer needle is equally distributed on both sides of the needle. The largest horizontal area around the tip is achieved by the 3-channel needle.

Conclusion: The tip configuration and number of channels have an influence on the distribution of fluid. The bevelled needle directs the fluid and reaches larger depths compared with the 3-channel needle that gets more horizontal spread.

Keywords: hypodermic needle, fluid distribution, tip configurations, multi-channel needles

Introduction

Hypodermic steel needles are mainly used for transdermal drug delivery. However, the disposal of steel needles can be a problem, high temperature is needed for incineration and a large amount of dangerous waste is generated. In developing countries the reuse of needle it's also an issue, that promotes the spread of blood-borne diseases like hepatitis and HIV infections [1]. A possible solution to these challenges could be a polymer needle. The needles made of polymer are much easier to de-activate which makes them easier to dispose of.

Polymer needles can be made with two or more channels allowing simultaneous delivery of reactive agents such as two component chemotherapy. This provides more precise medication once active components can be injected with high accuracy. Thus, polymer needles enable the innovation of new medical treatments and improved quality of existing treatments. However, it is important to understand how the new type of needles affects the distribution of fluid in tissue.

Cooley and Robison made experiments to investigate if the belief of some dentists that the bevel side of needles should face the bone when giving anesthesia was true [2]. They used 27G and 30G needles to inject a radiopaque solution in a segment of bovine muscle tissue to simulate what might occur in human tissue. The radiograph allows evaluate if the direction of bevel affect the direction of fluid. The result was two fluid deposition patterns. In the first pattern, an elongated pattern was deposited following the tissue planes, and the second pattern showed an oval distribution of the fluid around the tip of the needle. In both cases the fluid was deposited in approximately equal quantity on each side of the bevel. Thus, they concluded that the direction of the bevel did not affect the pattern of the fluid in the tissues and the belief of orienting the bevel toward the bone could not be justified.

The investigation of Juul and colleagues had as main goal to observe the deposition depth in the tissue using needles with different diameters and lengths: a 34G x 3 mm, a 32G x 5mm and a 30G x 8mm [3]. They made injections with each needle in *ex vivo* porcine tissue. 400 µL of a mixture with 70% insulin and 30% of contrast medium with 1mg/mL Alcian blue was delivered. As expected, the deposition volume peaked close to the depth corresponding to the needle tip for all needles. Measuring the distance between the tip of the needle and the lowest layer in the tissue with liquid, the 34G needle present the interval of depth from 3-12mm, the 32G from 5-14 mm and the 30G from 8-19mm, i.e. deposition depth varied with type and length of needle. All injections were deposited in the target tissue, the subcutaneous layer. Intra muscular injections are undesirable due to increased insulin absorption and risk of hypoglycemia. Regarding fluid distribution, they observed for all needles that the injected volume was along the connective tissue septae and not across lobules or fat cells. The fluid follows routes with less mechanical resistance in the local tissue. This study shows the importance of liquid distribution. The fluid should end up in the intended layer and neither lower in the muscle nor higher in the dermis. This could argue for using needle tips that encourage more horizontal fluid distribution.

The previous studies only investigated the use of thin standard needles in tissues. Thus, the aim of the present study is to investigate if the spread behaviour is different when needles with different tips and different number of channels were used (18G with bevel tip, 18G with blunt ending and polymer needle with 3 internal channels and conical tip). Bigger needles allowed us to observe what happens on spread of fluid on a larger scale. An artificial skin model was used to better understand the influence of different configurations of needles on distribution of fluid.

Artificial skin model

The skin from cadavers or animals could have been used to study materials-skin interactions. However, experiments using this type of models raise ethical issues and economic questions and they are characterized by variability since it is difficult to reproduce with the same conditions. For that reason, artificial skin models are often preferable. Another advantage is the reproducibility and reliability due to their simple and standardized construction. Therefore, these models represent lower costs, easy storage and manipulation. The artificial models can mimic one or more properties, functions or behaviour of the skin but are not capable to representing the multitude of in vivo skin properties [4, 5].

The development or adoption of an artificial skin model depends on the applications. Accordingly, there exist a multitude of artificial skin models and materials applied.

Dąbrowska and colleagues presented a range of materials that can simulate a specific physical propriety of the human skin [4]. To mimic the mechanical properties of the skin, materials such as gelatine and polyurethanes can be used.

The solution of water-gelatine had a similar density and viscosity as human tissue. Regular or ballistic gelatine have been used in earlier skin models. However, for our purpose the gelatine is not a good material because it’s too dense and do not allow the spread of fluid.

Due to the viscoelastic properties polyurethane foam can be used for mechanical skin models. The material is stable and has tunable properties. The polyurethane sponges have earlier been used to simulate the human skin [4].

Whittle and research team used an open-cell polyurethane sponge covered by a silicone layer to simulate the skin and sub-dermal tissue [6]. The aim of the study was to develop a model of the biomechanical dynamics of blunt force, non- ballistic wounding, which allow to better understand the mechanism behind the traumatic end-results.

When the complexity of skin is not taken into account, a simple homogeneous material is suitable for the understanding of the basic mechanisms controlling passive transport though a membrane [5].

The polyurethane sponge was a promising material for this study, because the material has open-cells that are connected, resulting in a soft and porous material. The material was tested and it was observed that there is a spread of fluid after injection in the material. A cold foam of polyurethane with dimensions of 50x50x50 mm and density of 0.035 g/cm^3 was used.

The artificial skin model can be produced from a combination of materials to mimic more properties of skin. In order to increase the resistance of the fluid passage, the polyurethane sponge was mixed with gelatin. However, the foam – gelatin combination showed a similar spread behavior compared with the polyurethane foam without gelatin. Therefore, cold foam polyurethane without gelatine was chosen for the fluid distribution tests.

To verify the similarity between the artifcial model and tissue, a test in *ex vivo* porcine tissue was made, see Figure 1. A tissue from the back of pig was used. The test consisted on injecting 0.1 ml and 0.2 ml of blue coloured fluid in sub-dermal tissue using a 18G needle. The spread results in this tissue, when 0.1ml was injected, was similar to the results obtained from the cold foam polyurethane model. When the volume was increased, it was observed that the fluid follow routes with less resistance and started to flow towards the outside by the lateral parts.

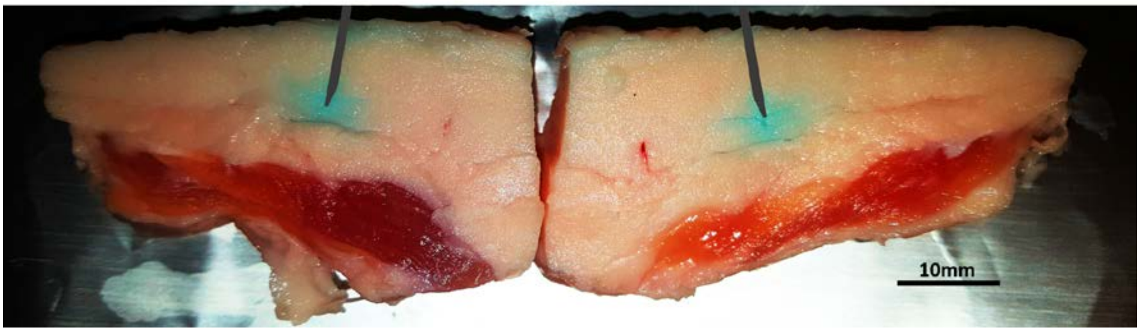

Figure 1: Test in ex vivo porcine tissue. The needle's drawing illustrates where the needle was placed and the spread of fluid can be seen around the tip.

Material and Methods

In order to evaluate the spread of fluid in a skin model a steel needle (BD Microlance 18G 1.2x40mm) and a polymer needle with 3 internal channels were selected. These needles were attached in the tip of a B-Braun Omnifix – F syringe which was filled with 0.3mL of fluid - a blue food dye mixed with ethanol. Ethanol evaporated quickly making it easier to slice the foam skin model without harming the distribution pattern. To validate the fluid distribution pattern another sponge was injected with blue coloured water and immediately dipped into floating nitrogen to freeze the water and sliced. The fluid was injected into the model using an Instron machine 3343 to compress the plunger of a syringe with constant velocity 2mm/s.

The artificial skin model described above was used. To ensure an even insertion direction a fixture was design in CAD and 3D printed. The fixture holds the syringe and the model as shown in Figure 2a. The fixture keeps the syringe and needle centred and restricts any lateral movement.

All experiments were done in triplicate. In the first set of experiments, the needle was used as received. On the second set of experiments, the bevel tip of 18G needle was removed by polishing it on a DP- U2 grinding drum machine. A 3-channels polymer needle with a conical tip was attached on a luer connector. Table 1 presents the dimensions of each needle. The dimensions were obtained from microscope images. The cross section area for the three channels in the polymer needle is similar to the cross section area of the steel needle cavity. Figure 3 shows the cross section and proportion of the dimensions between the 3-channel needle, the blunt and the bevelled needle.

Table 1: The dimensions and cross-section area for the fluid guiding channels in the 3 needles.

	Bevelled needle	**Blunt needle**	**3-channel needle**
Outer diameter d_e(mm)	1.26	1.26	2.15
Inner diameter d (mm)	0.90	0.90	-
Total cross-section area (mm^2)	0.64	0.64	0.67
Length L (mm)	37	33	34

The model was marked with an arrow to show the direction of the bevel in the first set of experiments as shown in Figure 2a. Figure 2b shows the marks indicating the orientation of the holes for the 3-channel needle and where the model is sliced.

After the test was performed, the model was removed from the fixture and sliced into two pieces with a sharp knife. The slicing is done along the insertion axis and pictures were taken for both halves of the model (left and right halves). To document the insertion path of the needle, a drop of purple ink was placed on the insertion spot. After needle insertion, a track can be seen in the foam which makes it possible to measure the area of fluid spread on each side of the needle. The depth (D) is measured from the uppermost open point in the needle to the lowest point of fluid in the model, see Figure 4. The open source Image J software was used to analyse the pictures and calculate the spread area and depth of fluid. This is used to estimate the ratio between the two sides of the needle (a and b) [7–9].

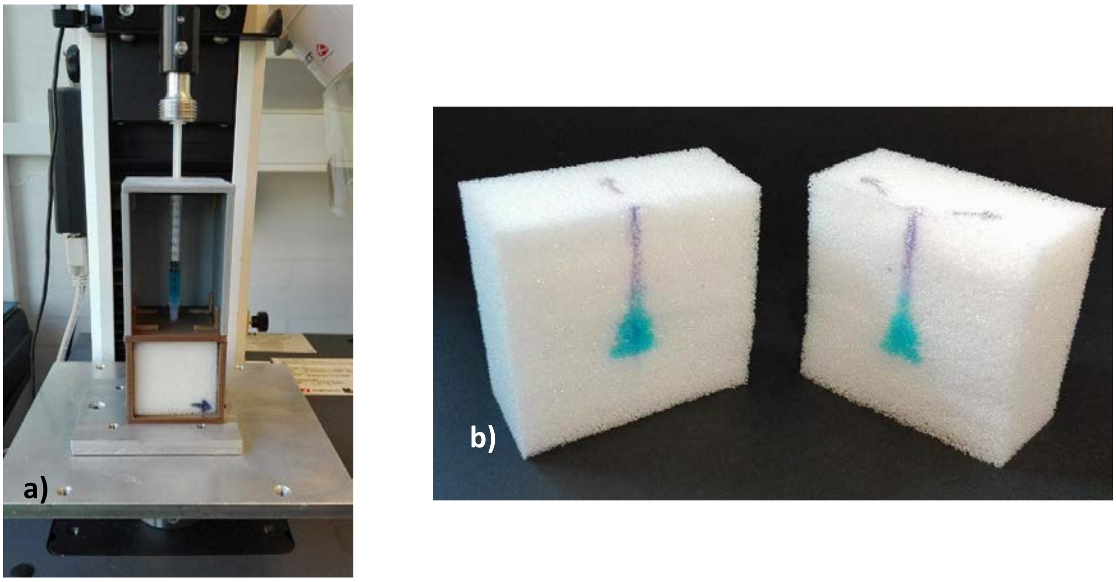

Figure 2: a) The fixture to hold the syringe and the foam model, b) Sliced foam model after injection with 3-channel needle. Arrows indicate the holes' orientation.

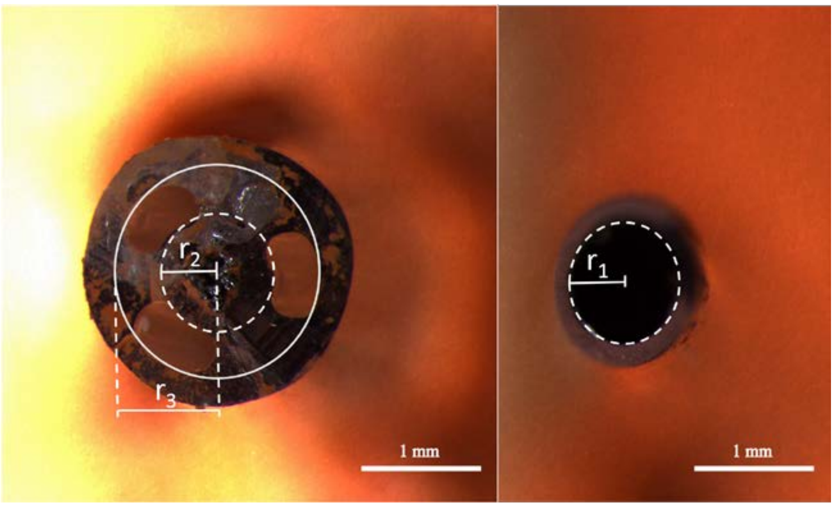

Figure 3: Proportions for the cross-section of a 3-channel needle (left) and the bevelled and blunt needle (right). r_1= *0.45mm,* r_2=*0.45mm and* r_3=*0.77mm.*

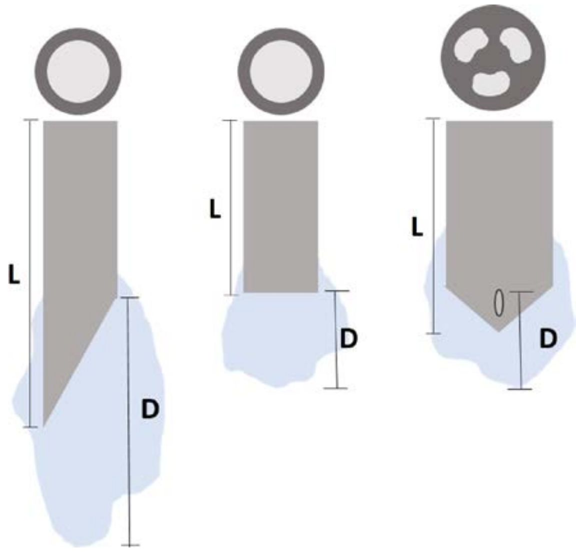

Figure 4: How depth is measured for each needle (bevelled and blunt steel needle and 3-channel needle) and their cross-section.

To analyse the spread around the tip of each needle a horizontal slice was made in the foam model in the plane of the needle tip. The Image J software was used to calculate the spread area around the tip.

Results

The following results present the spread area and the maximum depth achieved by fluid using a bevelled, a blunt and a 3-channel needle with conical tip.

The ratio (b/a) indicates which side of the needle the spread is largest. Values below 1 (b/a<1) indicate that the spread area is higher in the a side. Values higher than 1 indicate higher spread area on the b side, and b/a=1 means equal fluid distribution on each side of the needle.

Figure 5 shows examples of the experimental results for the three needles used. The first two columns illustrate the spread of fluid and the track of each needle shown for the left and the right halves of the model. The last two columns represent where the needle was placed and the orientation of the needle (a and b) for the two halves. This also makes it possible to observe the bevel direction for the bevelled needle.

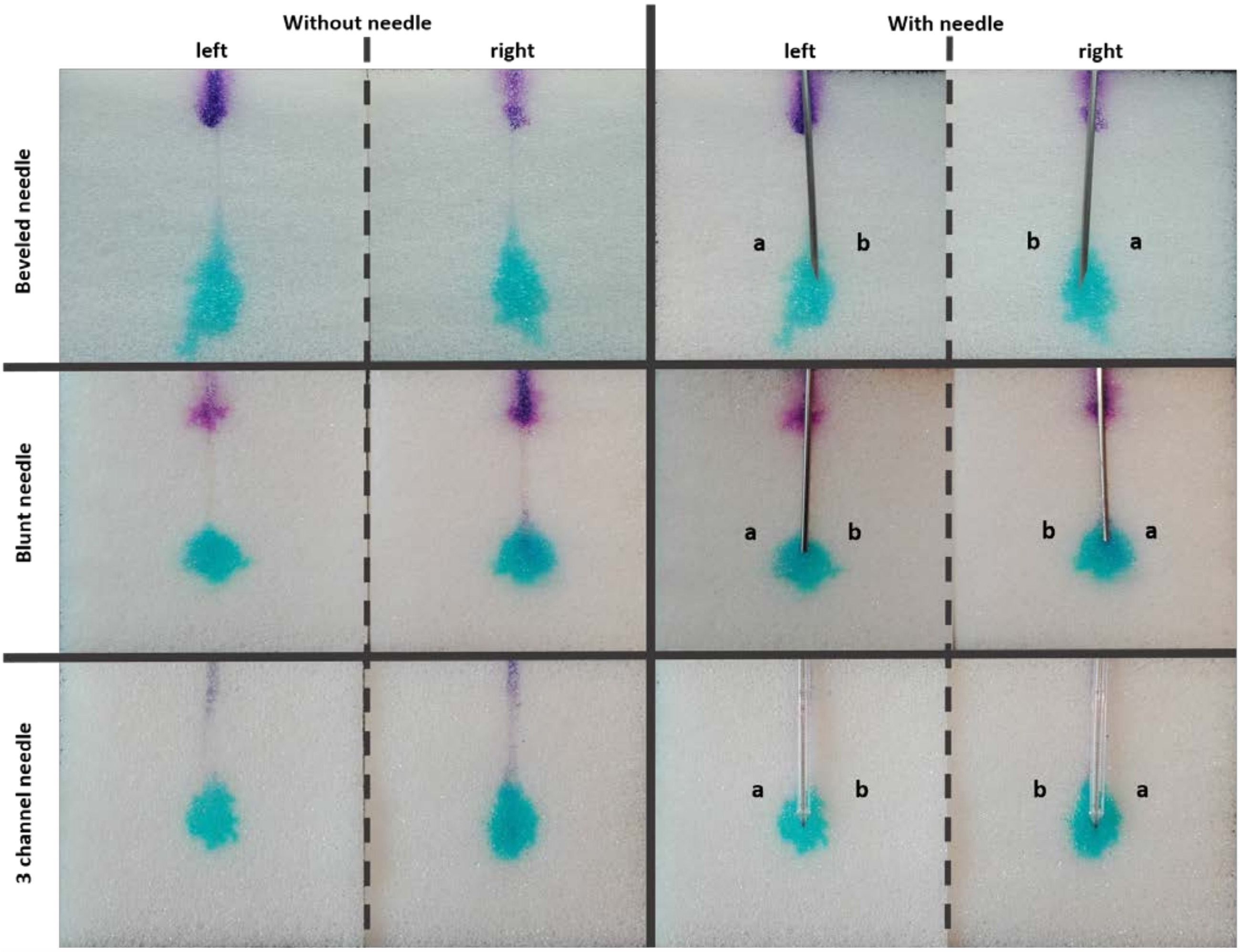

Figure 5:Experimental results. First row shows the results for bevelled needle, second row the results for the blunt needle and the last row the results for the 3-channel needle.

Table 2 shows the spread areas for the two sides of bevelled needle.

Table 2: Results for each experiment when using a bevelled needle including the area in front of the bevel, the area behind the bevel, the ratio between them and the maximum depth (D).

Experiments	Average		Ratio	
	Back side (b) (mm^2)	**Bevel side (a) (mm^2)**	**b/a**	**D (mm)**
1	21.51	49.15	0.44	11.28
2	44.15	70.90	0.62	13.69
3	33.06	51.40	0.64	12.69
Average	32.91	57.15	0.57	12.55

The b/a ratio lies between a 0.44 and 0.64 indicating that the fluid distributes easier in the direction of the bevel (a).

The maximum depth reached by the fluid is between 11.28 mm and 13.69 mm.

Table 3 shows the spread areas and the ratio for the two sides of the blunt needle.

Table 3: Results for the blunt needle including the spread area on each side of the needle, the ratio between them and the maximum depth (D) reached by the fluid.

Experiments	Average		Ratio	
	b(mm^2)	a(mm^2)	b/a	D (mm)
1	35.68	34.33	1.04	7.30
2	36.46	32.48	1.12	8.60
3	36.66	33.92	1.08	7.01
Average	36.27	33.58	1.08	7.64

The spread area on each side of the blunt needle is almost equal with a ratio (b/a) close to 1. However, in one of the experiments ratio was 1.12 showing that the fluid went a bit more for b side. The maximum depth achieved by the fluid lies between 7.30 mm and 8.60 mm.

The spread area for each side of the 3-channel needle (a and b) for each experiment can be seen in table 4.

Table 4: Results using the 3-channel needle: The spread area for each side of the needle, the ratio between them and the maximum depth (D) of the fluid.

Experiments	Average		Ratio	
	b(mm^2)	a(mm^2)	b/a	D (mm)
1	52.66	51.92	1.01	6.15
2	33.75	31.25	1.08	7.43
3	47.01	48.84	0.96	8.17
Average	44.47	44.00	1.02	7.25

The spread area for the polymer needle is almost equal for both sides of the needle with a ratio (b/a) of approximately 1.

The depth for the polymer needle ranges from 6.15 mm until 8.17 mm.

Figure 6 shows the horizontal spread of fluid around the needle tip and its shape measured at the top of the needle cavity opening.

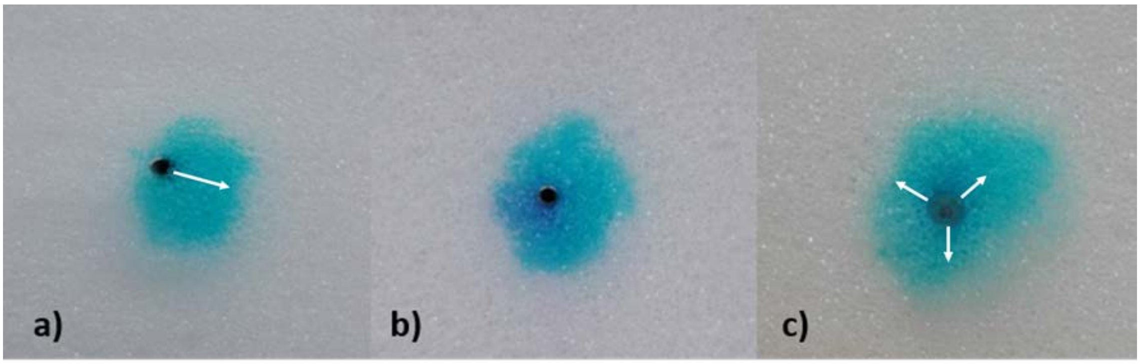

Figure 6: Shape of horizontal spread around the tip measured at the top of the needle cavity opening. a) bevelled needle (arrow indicates the direction of the bevel); b) blunt needle; c) 3-channel needle (arrows indicate the direction of each channel).

Table 5 shows the horizontal spread area around the tip of the 3 type of needle tips measured at the top of the needle cavity opening.

Table 5: Total horizontal spread area around the tip for each needle measured at the top of the needle cavity opening.

	Bevelled tip needle	**Blunt needle**	**3-channel needle**
Total area (mm^2)	55.72	66.39	95.68

It can be seen that a blunt needle can achieve higher horizontal spread area compared to a bevelled needle but the 3-channel needle performs best with a total spread area around the tip that is much higher than the two other needles shapes. However, the 3-channel needle had a larger diameter than the other two needles. The channels are placed farther from the centre which can cause a wider spread. To estimate the effect of this difference the expected spread of fluid was estimated assuming that the channels were moved in such a way, that their external boundary stays inside of the outer diameter of the other two steel needles. Thus, the channels were moved 0.32mm towards the centre. The spread area around the tip was 95.68 mm^2 which correspond to a circle with a radius of 5.52 mm. Assuming that the radial spread distance will be the same, when moving the channels 0.32 mm towards the centre, the new circle has a radius of 5.20 mm which correspond to an expected spread area around the tip of 84.91mm^2. This result is still larger than for the bevelled and blunt needle.

Discussion

The experimental data showed that the fluid distribution for a bevelled needle is biased to the side the bevel points (side a), i.e. $b/a<1$. The blunt needle and conical 3-channel needle have similar behaviour to each other, where the fluid is equally distributed in both sides of the needle, i.e. $b/a\approx1$.

This is in contrast to the study made by Cooley and Robison, which concluded that the direction of the bevel did not affect the pattern of the fluid in the tissue [2]. Possible explanations could be the size of the needle and the used tissue model. In the current study, a fairly thick needle (18G) and a foamed polymer tissue model were used, while Cooley and Robison used thinner needles (27G and 30G) and a segment of bovine muscle tissue. The muscle fibres in the animal tissue could be a stronger factor directing the injected liquid.

Concerning the depth of the fluid expelled by a bevelled needle it reached a larger depth (13.69 mm) than the blunt needle (8.60 mm) and the 3-channel needle (8.17 mm). The difference between the bevelled needle and the other two needles was approximately 40%. The blunt needle and the 3-channel needle had similar behaviour in terms of depth with only 5% difference.

The explanation for the differences in depth could be the presence of the bevel, which acts as a guide for the fluid. This means, when the fluid passes through the needle, some of it is guided by the bevel until its end, promoting a deeper distribution. For the blunt needle there is no guide and the liquid is distributed in more directions. The conical 3-channel needle also has a guide like the bevelled needle, but the dimensions are smaller and the liquid is guided in three directions.

The investigation by Juul and colleagues concluded that the deposit depth varies with the needle size and length. The fluid for 34G x 3mm and 32G x 5mm reach 9mm and for a 30G x 8mm reach a depth of 11mm, measuring the depth between the tip of the needle and the lowest layer in the tissue with liquid [3]. So, when the size and length of the needles are increased the fluid reaches further down. In our experiments, a bevelled 18G x37mm was used. Since the used needle presents a higher diameter and length than the ones used by Juul et al., it was expected to achieve a higher depth. The fluid reached a depth of 13.7mm and therefore complies with the previous results.

Regarding the horizontal spread area around the tip of the needle, the blunt needle had a spread area 16% higher than a bevelled needle which corresponds with a larger injection depth for the bevelled needle as was described above.

For the 3-channel needle, the horizontal spread area around the tip is much higher than for the other two needles. The difference between the 3-channel and the bevel needle is ca. 40% and ca. 30% between the 3-channel needle and the blunt needle. This difference can be explained by the presence of the 3 internal channels and the bevel like tip shape resulting from the conical tip. The 3-channel needle has 3 different places to expel the fluid while the bevel needle expel in only a single place. The other reason can be the proportion of dimension between the needles. In Table 1, it is possible to observe, that the bevelled and blunt needle (0.64 mm^2) and the 3-channel needle (0.67 mm^2) have similar cross section internal area where the fluid goes through. However, comparing the dimensions in the cross-sections as illustrated in Figure 3Figure 3: Proportions for the cross-section of a 3-channel needle (left) and the bevelled and blunt needle (right)., the radius of a circle around the 3 internal channels of the polymer needle is 0.32mm larger when comparing with the inner diameter of the channel for the bevelled and blunt needle. Thus, the 3-channel needle covers a larger area around the tip. If the 3-channel needle had the same outer dimension as the bevelled/blunt needle, which can be estimated by moving the channels 0.32mm towards the centre, this would result in a reduction of the spread area by 11%, when compared with the original configuration. However, the spread area around the tip is still much higher than the blunt and bevelled needle. The difference between the 3-channel needle with moved inner channels and the bevelled and the blunt needle would be 34% and 22%.

Conclusion

This study has investigated the fluid distribution in an artificial tissue model made from foamed polymer when injecting with a bevelled needle, a blunt needle and a needle with 3 internal channels and conical tip. The results indicated that the bevel tip had an influence on the fluid distribution in contrast to earlier findings. The bevelled needle directed the fluid and reached a larger depth. The spread of fluid using a 3-channel needle and a blunt needle was equally distributed in both sides of needles and reached almost similar depths. These two needles provided 40% less fluid depth compared to the bevelled needle. The 3-channel needle provided a better horizontal spread of liquid around the tip. When the 3-channel needle had the same outer diameter as the bevelled/blunt needle, the spread area of the 3-channel needle was 34% and 22% larger compared with the bevelled and blunt needles.

Acknowledgement

We are grateful to professor Rajan Ambat for kindly providing access to materials testing facilities.

References

1. Busillo, E., Colton, J.S.: Characterization of Plastic Hypodermic Needles. J. Med. Device. 3, 41004 (2009).
2. Cooley, R.L., Robison, S.F.: Comparative evaluation of the 30-gauge dental needle. Oral Surgery, Oral Med. Oral Pathol. 48, 400–404 (1979).
3. Juul, K.A.P., Bengtsson, H., Eyving, B., Kildegaard, J., Lav, S., Poulsen, M., Serup, J., Stallknecht, B.: Influence of hypodermic needle dimensions on subcutaneous injection delivery - a pig study of injection deposition evaluated by CT scanning, histology, and backflow. Ski. Res. Technol. 18, 447–455 (2012).
4. Dąbrowska, A.K., Rotaru, G.-M., Derler, S., Spano, F., Camenzind, M., Annaheim, S., Stämpfli, R., Schmid, M., Rossi, R.M.: Materials used to simulate physical properties of human skin. Ski. Res. Technol. 22, 3–14 (2016).
5. Abd, E., Yousef, S.A., Pastore, M.N., Telaprolu, K., Mohammed, Y.H., Namjoshi, S., Grice, J.E., Roberts, M.S.: Skin models for the testing of transdermal drugs. Clin. Pharmacol. Adv. Appl. 8, 163–176 (2016).
6. Whittle, K., Kieser, J., Ichim, I., Swain, M., Waddell, N., Livingstone, V., Taylor, M.: The biomechanical modelling of non-ballistic skin wounding: Blunt-force injury. Forensic Sci. Med. Pathol. 4, 33–39 (2008).
7. Schneider, C.A., Rasband, W.S., Eliceiri, K.W.: NIH Image to ImageJ: 25 years of image analysis. Nat. Methods. 9, 671–675 (2012).
8. Schindelin, J., Rueden, C.T., Hiner, M.C., Eliceiri, K.W.: The ImageJ ecosystem: An open platform for biomedical image analysis. Mol. Reprod. Dev. 82, 518–529 (2015).
9. Rasband, W.S.: ImageJ, https://imagej.net.

Address:

Silvana Gomes
Technical University of Denmark,

Dept. of Mechanical Engineering,
Produktionstorvet b. 426B
DK-2800 Kgs. Lyngby,
Denmark.
Tel: + 4545254811
e-mail: silvanagomes311@gmail.com